Supplementary Information

Local Chromatin Organization and Net Charge Modulate DNA Glycosylase Efficiency in Live Cells

Jingfang Zhao[1], Jingwen Deng[1], Zhe Zhao[1,6], Quan Yuan[2], Weihua Huang[2], Li-Sheng Zhang[4], Shuoxing Jiang[5], Miao Yu[3], Guohong Li[3], Ke Xu[7], Limin Xiang[1]*

1. College of Chemistry and Molecular Sciences, State Key Laboratory of Metabolism and Regulation in Complex Organisms, College of Life Sciences, Taikang Center for Life and Medical Sciences, Wuhan University, Wuhan, China 430072

2. College of Chemistry and Molecular Sciences, Wuhan University, Wuhan, China 430072

3. State Key Laboratory of Metabolism and Regulation in Complex Organisms, College of Life Sciences, Taikang Center for Life and Medical Sciences, Wuhan University, Wuhan, China 430072

4. Department of Chemistry and Division of Life Science, The Hong Kong University of Science and Technology (HKUST), Kowloon 999077 Hong Kong SAR, China

5. State Key Laboratory of Coordination Chemistry, Department of Biomedical Engineering, College of Engineering and Applied Sciences, Nanjing University, Nanjing, Jiangsu 210023, P. R. China

6. Department of Physics, University of Muenster, Muenster, 48159, Germany

7. Department of Chemistry, University of California, Berkeley, California, United States 94720

*Corresponding author. limin.xiang@whu.edu.cn

The PDF file includes:

Extended Data Figures 1-6

Extended Data Table 1

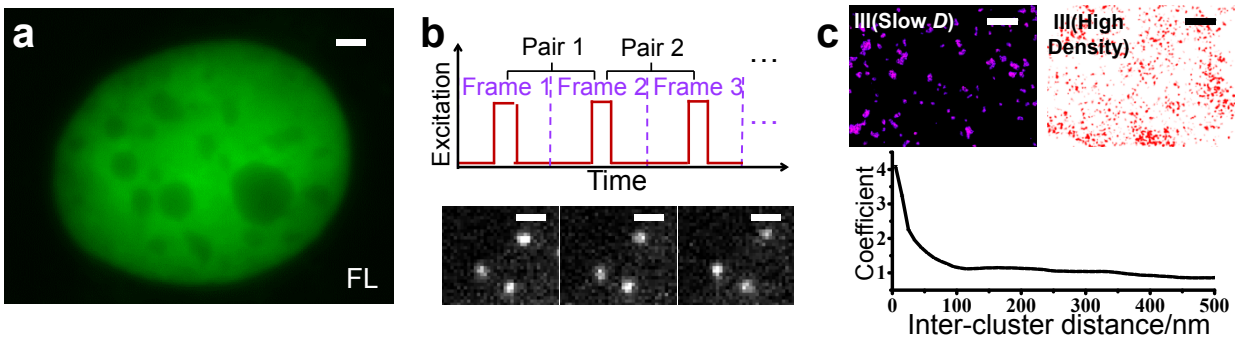

Extended Data Figure 1 | Single-molecule diffusivity mapping of human 8-oxoguanine DNA glycosylase (hOGG1) in live cell nuclei.

a). Epifluorescence (FL) image of hOGG1 in live cell nuclei.

b). Single molecules of mEOS3.2-tagged hOGG1 were excited using stroboscopic illumination and tracked between consecutive frames. The illumination time was ~2 ms, and the separation time between consecutive frames was ~6 ms.

c). Cross-correlation analysis between slow-diffusion clusters (left) and high-density clusters (right) in Region III of Figure 1g revealed a strong correlation, suggesting that slow-diffusion clusters likely represent tight bindings with chromatin.

Scale bar: 2 μm in **a**, 1 μm in **b**, 500 nm in **c**.

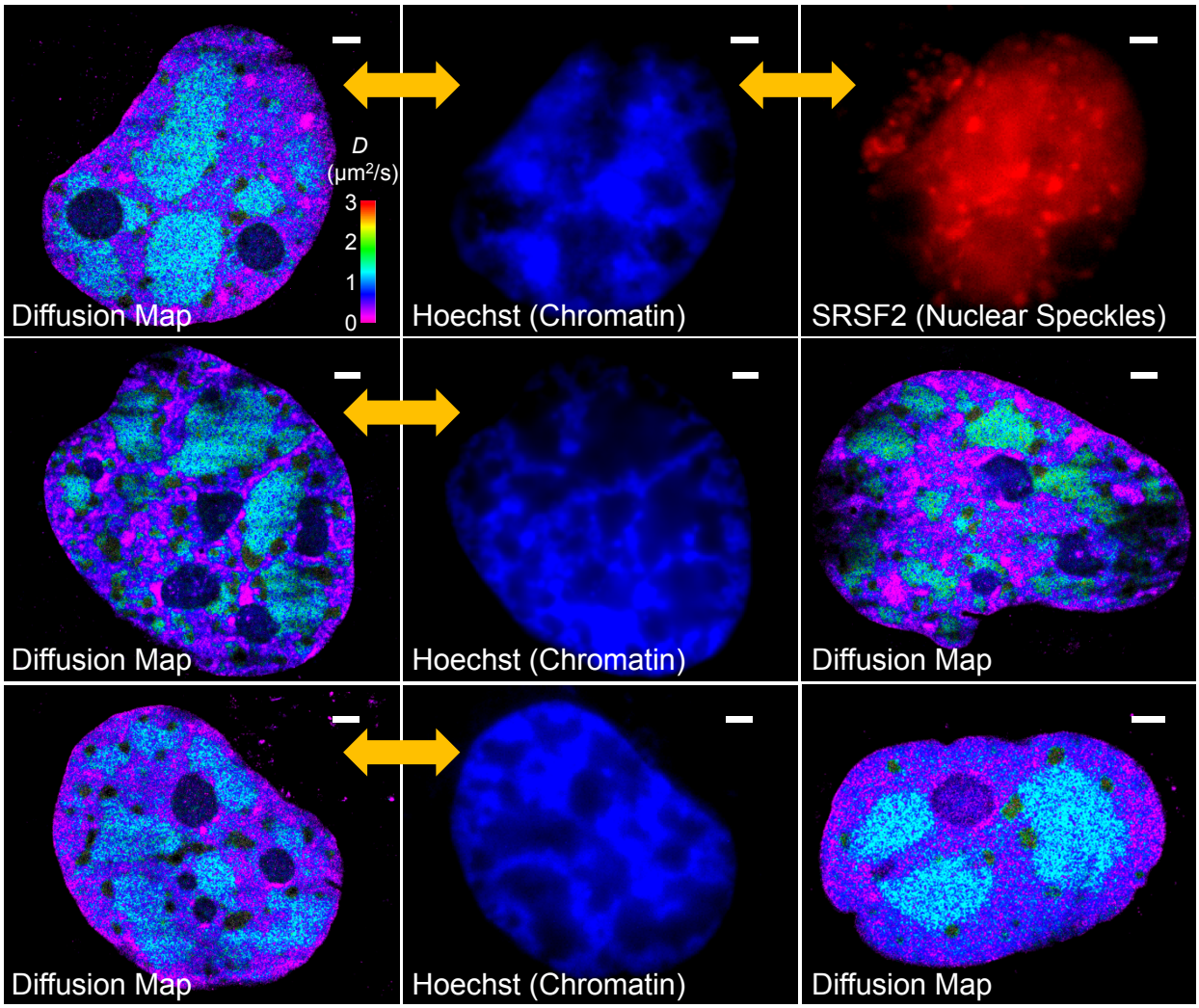

Extended Data Figure 2 | Additional pc-SM*d*M diffusion maps of hOGG1 in live cells. Representative images showing four distinct diffusion regions, along with correlative images stained with Hoechst (chromatin) and SRSF2 (nuclear speckles), indicated by arrows. *Scale bar*: 2 μm. The diffusion rate color scale is consistent across all panel.

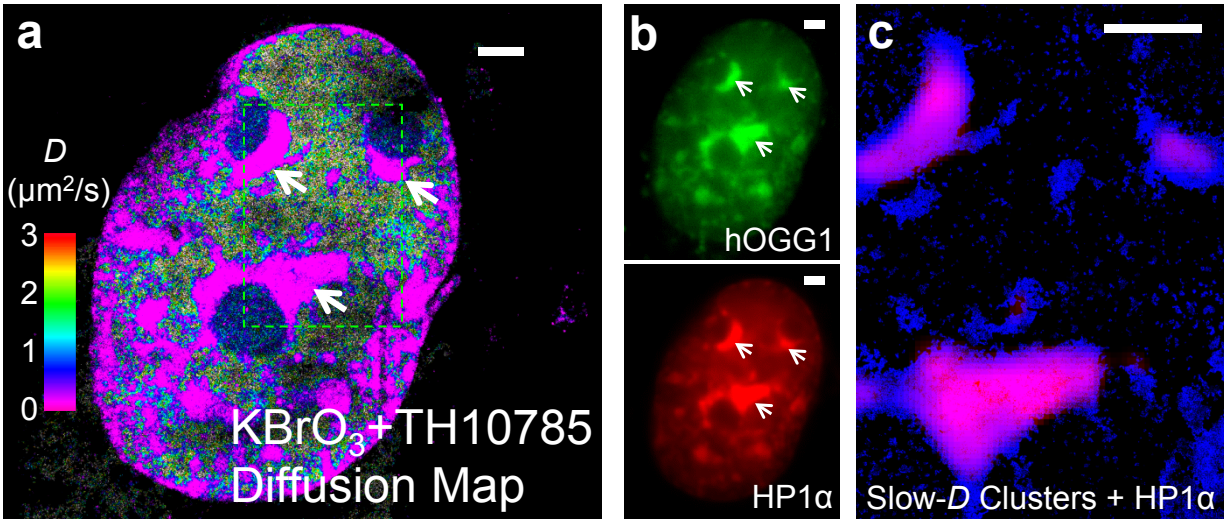

Extended Data Figure 3 | Correlative pc-SM*d*M diffusion maps of hOGG1 and epifluorescence image of HP1α

a). pc-SM*d*M image of hOGG1 after activator treatment and co-expression of iRFP702-tagged HP1α.

b). Epifluorescence images of mEOS3.2-tagged hOGG1 (top) and iRFP702-tagged HP1α (bottom), corresponding to panel **a**. Heterochromatin closely correlates with the condensates formed by hOGG1 (white arrows).

c). Overlay of slow-diffusing clusters (blue) and HP1α (red) suggesting condensates form both within and around heterochromatin (corresponding to the green box in panel **a**).

Scale bar: 2 μm.

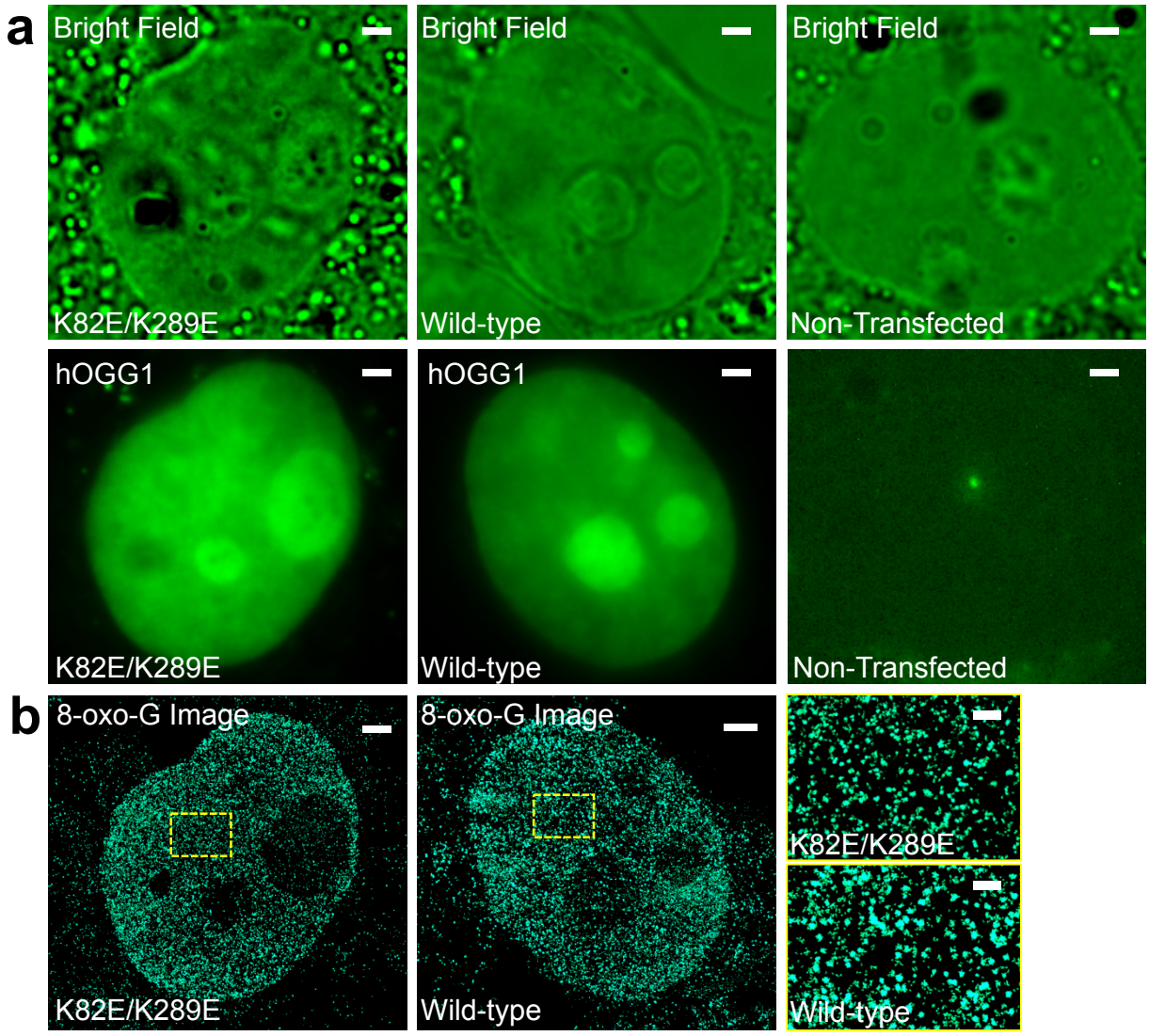

Extended Data Figure 4 | DNA-PAINT imaging of 8-oxo-G in nuclei of cells with and without transfection.

a). Bright-field images (top) and epifluorescence images (bottom) of cells transfected with the K82E/K289E mutant (left, corresponding to Figure 5i), transfected with wild-type hOGG1 (middle), and without transfection (right, corresponding to Figure 5h).

b). Comparison of DNA-PAINT images of 8-oxo-G in nuclei of cells transfected with K82E/K289E (left) and wild-type hOGG1 (right). Zoom-in images revealed lower 8-oxo-G cluster density in cells expressing K82E/K289E compared to wild-type hOGG1, indicating improved repair efficiency in the mutant.

Scale bar: 2 μm in **a**, left and middle panel of **b**. 500 nm in right panel of **b**.

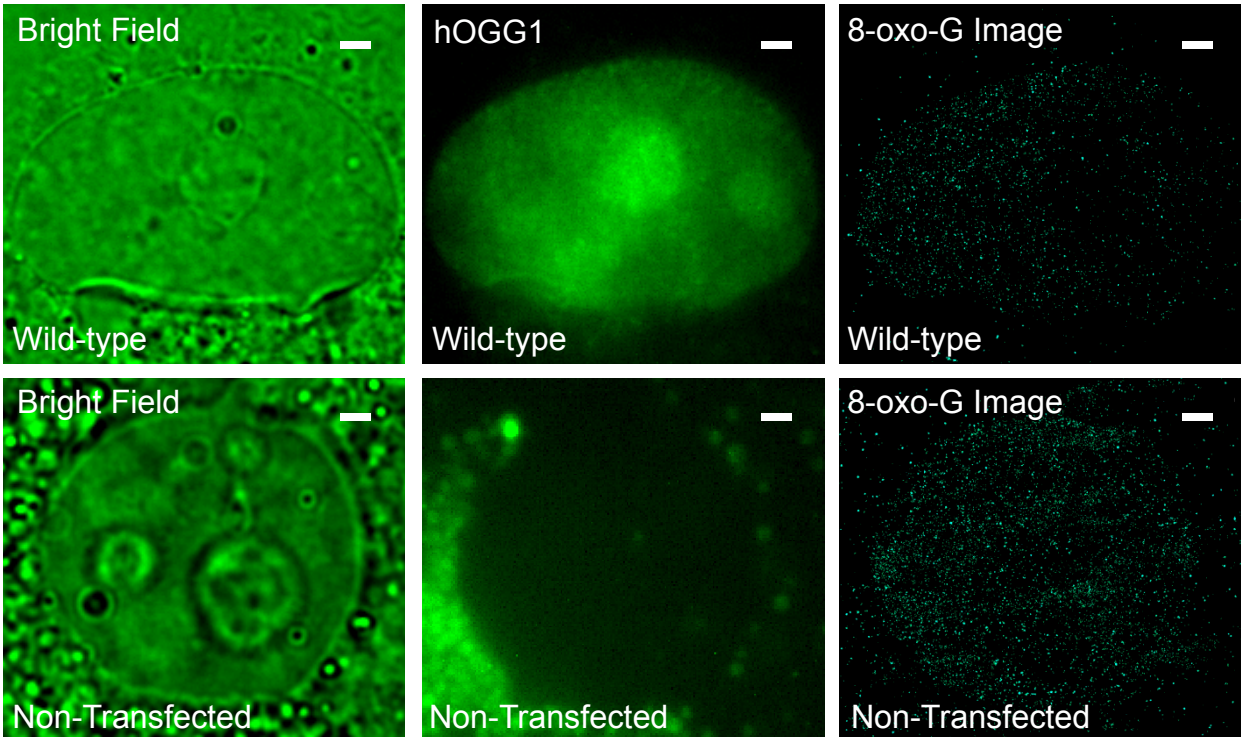

Extended Data Figure 5 | Bright-field (left), epifluorescence (middle), and DNA-PAINT images of 8-oxo-G (right) in nuclei of cells with and without transfection in the <u>ABSENCE</u> of the aptamer-docking strand. As a control experiment to Figures 5h and 5i, these images show significantly fewer 8-oxo-G clusters in the nuclei without the aptamer binding.
Scale bar: 2 μm.

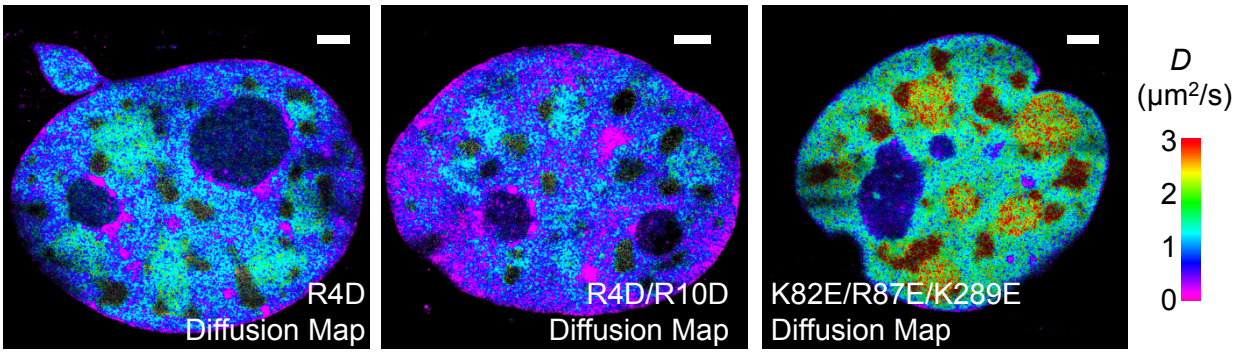

Extended Data Figure 6 | Diffusion rates of mEOS3.2-hOGG1 variants with mutations in specific positively charged residues that failed to exhibit faster diffusion rates. The diffusion rates of R4D and R4D/R10D were compared to wild-type mEOS3.2-hOGG1, while the diffusion rates of K82E/R87E/K289E were compared to the K82E/K289E variant.

Scale bar: 2 μm. Diffusion rate color scale is consistent across all panels.

Extended Data Table 1 | The sequences and predicted charges of the all the plasmids used in this work

Name	Full Sequences. Mutants were highlighted in red (for negatively charged amino acids) or blue (for other amino acids).	Charge pH=7.4
hOGG1	MPARALLPRRMGHRTLASTPALWASIPCPRSELRLD LVLPSGQSFRWREQSPAHWSGVLADQVWTLTQTEE QLHCTVYRGDKSQASRPTPDELEAVRKYFQLDVTL AQLYHHWGSVDSHFQEVAQKFQGVRLLRQDPIECL FSFICSSNNNIARITGMVERLCQAFGPRLIQLDDVTY HGFPSLQALAGPEVEAHLRKLGLGYRARYVSASAR AILEEQGGLAWLQQLRESSYEEAHKALCILPGVGTK VADCICLMALDKPQAVPVDVHMWHIAQRDYSWHP TTSQAKGPSPQTNKELGNFFRSLWGPYAGWAQAVL FSADLRQSRHAQEPPAKRRKGSKGPEG	+6.6; pI = 8.61
mEOS3.2	MSAIKPDMKIKLRMEGNVNGHHFVIDGDGTGKPFE GKQSMDLEVKEGGPLPFAFDILTTAFHYGNRVFAKY PDNIQDYFKQSFPKGYSWERSLTFEDGGICNARNDIT MEGDTFYNKVRFYGTNFPANGPVMQKKTLKWEPST EKMYVRDGVLTGDIEMALLLEGNAHYRCDFRTTYK AKEKGVKLPGAHFVDHCIEILSHDKDYNKVKLYEH AVAHSGLPDNARR	+0.5; pI = 7.56
hOGG1-mEOS3.2 (611 AAs)	MAQVQLQVDMPARALLPRRMGHRTLASTPALWASI PCPRSELRLDLVLPSGQSFRWREQSPAHWSGVLADQ VWTLTQTEEQLHCTVYRGDKSQASRPTPDELEAVR KYFQLDVTLAQLYHHWGSVDSHFQEVAQKFQGVR LLRQDPIECLFSFICSSNNNIARITGMVERLCQAFGPR LIQLDDVTYHGFPSLQALAGPEVEAHLRKLGLGYRA RYVSASARAILEEQGGLAWLQQLRESSYEEAHKALC ILPGVGTKVADCICLMALDKPQAVPVDVHMWHIAQ RDYSWHPTTSQAKGPSPQTNKELGNFFRSLWGPYA	+8.4; pI = 8.44

	GWAQAVLFSADLRQSRHAQEPPAKRRKGSKGPEGG PVATMSAIKPDMKIKLRMEGNVNGHHFVIDGDGTG KPFEGKQSMDLEVKEGGPLPFAFDILTTAFHYGNRV FAKYPDNIQDYFKQSFPKGYSWERSLTFEDGGICNA RNDITMEGDTFYNKVRFYGTNFPANGPVMQKKTLK WEPSTEKMYVRDGVLTGDIEMALLLEGNAHYRCDF RTTYKAKEKGVKLPGAHFVDHCIEILSHDKDYNKV KLYEHAVAHSGLPDNARRSGLRSRAQASNSAVDGT AGPGSTGSR	
K249Q-hOGG1	MPARALLPRRMGHRTLASTPALWASIPCPRSELRLD LVLPSGQSFRWREQSPAHWSGVLADQVWTLTQTEE QLHCTVYRGDKSQASRPTPDELEAVRKYFQLDVTL AQLYHHWGSVDSHFQEVAQKFQGVRLLRQDPIECL FSFICSSNNNIARITGMVERLCQAFGPRLIQLDDVTY HGFPSLQALAGPEVEAHLRKLGLGYRARYVSASAR AILEEQGGLAWLQQLRESSYEEAHKALCILPGVGTQ VADCICLMALDKPQAVPVDVHMWHIAQRDYSWHP TTSQAKGPSPQTNKELGNFFRSLWGPYAGWAQAVL FSADLRQSRHAQEPPAKRRKGSKGPEG	+5.6; pI = 8.46
H270A-hOGG1	MPARALLPRRMGHRTLASTPALWASIPCPRSELRLD LVLPSGQSFRWREQSPAHWSGVLADQVWTLTQTEE QLHCTVYRGDKSQASRPTPDELEAVRKYFQLDVTL AQLYHHWGSVDSHFQEVAQKFQGVRLLRQDPIECL FSFICSSNNNIARITGMVERLCQAFGPRLIQLDDVTY HGFPSLQALAGPEVEAHLRKLGLGYRARYVSASAR AILEEQGGLAWLQQLRESSYEEAHKALCILPGVGTK VADCICLMALDKPQAVPVDVAMWHIAQRDYSWHP TTSQAKGPSPQTNKELGNFFRSLWGPYAGWAQAVL FSADLRQSRHAQEPPAKRRKGSKGPEG	+6.5; pI = 8.61
K82E/	MPARALLPRRMGHRTLASTPALWASIPCPRSELRLD LVLPSGQSFRWREQSPAHWSGVLADQVWTLTQTEE	+2.7; pI = 7.69

K289E-hOGG1	QLHCTVYRGDESQASRPTPDELEAVRKYFQLDVTLA QLYHHWGSVDSHFQEVAQKFQGVRLLRQDPIECLFS FICSSNNNIARITGMVERLCQAFGPRLIQLDDVTYHG FPSLQALAGPEVEAHLRKLGLGYRARYVSASARAIL EEQGGLAWLQQLRESSYEEAHKALCILPGVGTKVA DCICLMALDKPQAVPVDVHMWHIAQRDYSWHPTTS QAEGPSPQTNKELGNFFRSLWGPYAGWAQAVLFSA DLRQSRHAQEPPAKRRKGSKGPEG	
piRFP702-N1(Addgene #45456)	MARKVDLTSCDREPIHIPGSIQPCGCLLACDAQAVRI TRITENAGAFFGRETPRVGELLADYFGETEAHALRN ALAQSSDPKRPALIFGWRDGLTGRTFDISLHRHDGTS IIEFEPAAAEQADNPLRLTRQIIARTKELKSLEEMAAR VPRYLQAMLGYHRVMLYRFADDGSGKVIGEAKRSD LESFLGQHFPASLVPQQARLLYLKNAIRVVSDSRGIS SRIVPEHDASGAALDLSFAHLRSISPIHLEFLRNMGVS ASMSLSIIIDGTLWGLIICHHYEPRAVPMAQRVAAEM FADFLSLHFTAAHHQR	pI=7.25
SRSF2-iRFP702	MSYGRPPPDVEGMTSLKVDNLTYRTSPDTLRRVFEK YGRVGDVYIPRDRYTKESRGFAFVRFHDKRDAEDA MDAMDGAVLDGRELRVQMARYGRPPDSHHSRRGP PPRRYGGGGYGRRSRSPRRRRRSRSRSRSRSRSRSRS RYSRSKSRSRTRSRSRSTSKSRSARRSKSKSSSVSRSR SRSRSRSRSRSPPPVSKRESKSRSRSKSPPKSPEEEGA VSSGGAGGSTGRHMARKVDLTSCDREPIHIPGSIQPC GCLLACDAQAVRITRITENAGAFFGRETPRVGELLA DYFGETEAHALRNALAQSSDPKRPALIFGWRDGLTG RTFDISLHRHDGTSIIEFEPAAAEQADNPLRLTRQIIA RTKELKSLEEMAARVPRYLQAMLGYHRVMLYRFA DDGSGKVIGEAKRSDLESFLGQHFPASLVPQQARLL YLKNAIRVVSDSRGISSRIVPEHDASGAALDLSFAHL	pI=11.03

	RSISPIHLEFLRNMGVSASMSLSIIIDGTLWGLIICHHY EPRAVPMAQRVAAEMFADFLSLHFTAAHHQR	
NPM1- iRFP702	ATMEDSMDMDMSPLRPQNYLFGCELKADKDYHFK VDNDENEHQLSLRTVSLGAGAKDELHIVEAEAMNY EGSPIKVTLATLKMSVQPTVSLGGFEITPPVVLRLKC GSGPVHISGQHLVAVEEDAESEDEEEEDVKLLSISGK RSAPGGGSKVPQKKVKLAADEDDDDDDEEDDDED DDDDDFDDEEAEEKAPVKKSIRDTPAKNAQKSNQN GKDSKPSSTPRSKGQESFKKQEKTPKTPKGPSSVEDI KAKMQASIEKGGSLPKVEAKFINYVKNCFRMTDQE AIQDLWQWRKSLGGAGGDPPVATMARKVDLTSCD REPIHIPGSIQPCGCLLACDAQAVRITRITENAGAFFG RETPRVGELLADYFGETEAHALRNALAQSSDPKRPA LIFGWRDGLTGRTFDISLHRHDGTSIIEFEPAAAEQA DNPLRLTRQIIARTKELKSLEEMAARVPRYLQAMLG YHRVMLYRFADDGSGKVIGEAKRSDLESFLGQHFPA SLVPQQARLLYLKNAIRVVSDSRGISSRIVPEHDASG AALDLSFAHLRSISPIHLEFLRNMGVSASMSLSIIIDGT LWGLIICHHYEPRAVPMAQRVAAEMFADFLSLHFTA AHHQR	pI =5.28
CBX5- iRFP702(HP1α)	MGKKTKRTADSSSSEDEEEYVVEKVLDRRVVKGQV EYLLKWKGFSEEHNTWEPEKNLDCPELISEFMKKYK KMKEGENNKPREKSESNKRKSNFSNSADDIKSKKKR EQSNDIARGFERGLEPEKIIGATDSCGDLMFLMKWK DTDEADLVLAKEANVKCPQIVIAFYEERLTWHAYPE DAENKEKETAKSGGAGGGAGGDPPVATMARKVDL TSCDREPIHIPGSIQPCGCLLACDAQAVRITRITENAG AFFGRETPRVGELLADYFGETEAHALRNALAQSSDP KRPALIFGWRDGLTGRTFDISLHRHDGTSIIEFEPAAA EQADNPLRLTRQIIARTKELKSLEEMAARVPRYLQA MLGYHRVMLYRFADDGSGKVIGEAKRSDLESFLGQ	pI =6.49

	HFPASLVPQQARLLYLKNAIRVVSDSRGISSRIVPEH DASGAALDLSFAHLRSISPIHLEFLRNMGVSASMSLSI IIDGTLWGLIICHHYEPRAVPMAQRVAAEMFADFLS LHFTAAHHQR	
mEOS3.2- H2B	MSAIKPDMKIKLRMEGNVNGHHFVIDGDGTGKPFE GKQSMDLEVKEGGPLPFAFDILTTAFHYGNRVFAKY PDNIQDYFKQSFPKGYSWERSLTFEDGGICNARNDIT MEGDTFYNKVRFYGTNFPANGPVMQKKTLKWEPST EKMYVRDGVLTGDIEMALLLEGNAHYRCDFRTTYK AKEKGVKLPGAHFVDHCIEILSHDKDYNKVKLYEH AVAHSGLPDNARRSGLRSRALEFATMPEPSKSAPAP KKGSKKAITKAQKKDGKKRKRSRKESYSIYVYKVL KQVHPDTGISSKAMGIMNSFVNDIFERIAGEASRLAH YNKRSTITSREIQTAVRLLLPGELAKHAVSEGTKAVT KYTSSKLVDGTAGPGSTGSR	pI =9.74